
DIPPER: Direct Preference Optimization to Accelerate Primitive-Enabled Hierarchical Reinforcement Learning

Utsav Singh
CSE Deptt.
IIT Kanpur, India
utsavz@iitk.ac.in

Souradip Chakraborty
University of Maryland
College Park, MD, USA

Wesley A. Suttle
U.S. Army Research Laboratory
Adelphi, MD, USA

Brian M. Sadler
University of Texas
Austin, Texas, USA

Vinay P Namboodiri
CS Deptt.
University of Bath, Bath, UK

Amrit Singh Bedi
CS Deptt., University of Central Florida
Orlando, Florida, USA

Abstract

Learning control policies to perform complex robotics tasks from human preference data presents significant challenges. On the one hand, the complexity of such tasks typically requires learning policies to perform a variety of subtasks, then combining them to achieve the overall goal. At the same time, comprehensive, well-engineered reward functions are typically unavailable in such problems, while limited human preference data often is; making efficient use of such data to guide learning is therefore essential. Methods for learning to perform complex robotics tasks from human preference data must overcome both these challenges simultaneously. In this work, we introduce DIPPER: Direct Preference Optimization to Accelerate Primitive-Enabled Hierarchical Reinforcement Learning, an efficient hierarchical approach that leverages direct preference optimization to learn a higher-level policy and reinforcement learning to learn a lower-level policy. DIPPER enjoys improved computational efficiency due to its use of direct preference optimization instead of standard preference-based approaches such as reinforcement learning from human feedback, while it also mitigates the well-known hierarchical reinforcement learning issues of non-stationarity and infeasible subgoal generation due to our use of primitive-informed regularization inspired by a novel bi-level optimization formulation of the hierarchical reinforcement learning problem. To validate our approach, we perform extensive experimental analysis on a variety of challenging robotics tasks, demonstrating that DIPPER outperforms hierarchical and non-hierarchical baselines, while ameliorating the non-stationarity and infeasible subgoal generation issues of hierarchical reinforcement learning.

1 Introduction

Although deep reinforcement learning (RL) has driven significant progress in executing complex robotic manipulation tasks when rewards are available [34, 16, 11, 23], the success of RL in such domains is impeded due to challenges like ineffective exploration and long-term credit assignment, particularly in sparse-reward scenarios [28]. Hierarchical reinforcement learning [37, 9, 38, 18, 14] is an elegant framework which promises the benefits of temporal abstraction and improved exploration [27] to overcome these issues. In the goal-conditioned hierarchical RL setting [9, 38] that we consider in this paper, in particular, the higher-level policy provides subgoals to a lower-level

policy, which in turn tries to achieve those subgoals by executing primitive actions. Off-policy HRL approaches [24, 26] suffer from serious challenges, however, including: (i) non-stationarity in HRL due to the non-stationarity of lower-level policies, and (ii) infeasible subgoal generation by higher-level policies [5]. Fortunately, recent work leveraging primitive-informed regularization has been proposed that addresses both these issues [36].

While the foregoing provides hope that HRL methods can be leveraged while learning to perform complex robotics tasks from human preference data, the problem remains of how to efficiently incorporate human preferences. Recently, reinforcement learning from human feedback (RLHF), a subset of preference-based learning, has been proposed for learning control policies from human preference data [6, 15, 21]. In this setting, a reward model is first learned on an outer level from the human preference data, then RL is used on an inner level to train a policy to solve the task corresponding to the learned reward model. In light of this, a natural approach to the problem of learning policies for complex robotics tasks from human preference data is to combine RLHF and HRL, which effectively yields a three-tier approach: at the highest tier, a reward model is learned using human preference feedback; at the middle tier, RL is used to learn a corresponding higher-level policy by maximizing the reward model to predict subgoals for a lower-level policy; at the lowest tier, RL is used to optimize the lower-level policy to achieve the subgoals provided by the higher-level policy. However, implementing this elaborate, three-tier approach would be computationally challenging, and a suitable simplification is thus required. Fortunately, the recently proposed direct preference optimization (DPO) [33] approach circumvents the RLHF-specific need for both learning a reward model and performing RL by directly optimizing the policy with respect to a maximum likelihood objective capturing the human preference data. This raises the following question:

does there exist a hierarchical DPO approach for solving robotic control tasks from human preference data that simultaneously addresses the non-stationarity and infeasible subgoal issues in HRL?

In this work we answer this question in the affirmative by proposing DIPPER: **DI**rect **P**reference **O**ptimization to Accelerate **P**rimitive-Enabled **H**ierarchical **R**einforcement Learning. In DIPPER, the higher-level policy is learned from human preference data using a DPO objective, while the lower-level policy is learned using RL. The key insight behind the HRL component of DIPPER is that this formulation decouples the higher-level policy from the non-stationary lower-level primitive, which mitigates the non-stationarity issue in off-policy HRL. Additionally, to bridge the DPO and HRL components of DIPPER we derive a primitive-enabled reference policy inspired by a bi-level optimization formulation of the HRL problem that regularizes the higher-level policy to predict feasible subgoals for the lower-level policy. To the best of our knowledge, ours is the first approach that effectively combines hierarchical learning and DPO to learn policies for solving complex robotics tasks from human preference data. To validate the effectiveness of the proposed approach, we conduct experiments in a variety of challenging robotics tasks in which DIPPER demonstrates impressive performance and consistently outperforms existing baselines.

To summarize, the primary contributions of this work are as follows:

- (i) we propose a novel hierarchical formulation of DPO for solving complex robotic control tasks from human preference data (Section 4),
- (ii) we show that DIPPER is able to mitigate non-stationarity in off-policy HRL (Section 5),
- (iii) using our bi-level optimization formulation, we derive a primitive-enabled reference policy to condition the higher-level policy to generate feasible subgoals (Section 4.1.2),
- (iv) and we experimentally demonstrate that DIPPER achieves greater than 40% success rates in complex robotic control tasks where other baselines typically fail to show significant progress (Section 5).

2 Related Works

Hierarchical Reinforcement Learning. HRL provides an elegant framework that promises the benefits of improved exploration and temporal abstraction [27]. Due to this, multiple hierarchical approaches have been studied in literature [37, 2, 30, 10]. We consider a goal-conditioned setup in this work, where a higher-level policy provides subgoals to a lower-level policy, and the lower-level policy executes primitive actions directly on the environment. In this setup, multiple prior approaches have been proposed [9, 38]. Although it promises these intuitive benefits, HRL has been cursed with multiple issues like non-stationarity in off-policy HRL, when multiple levels are

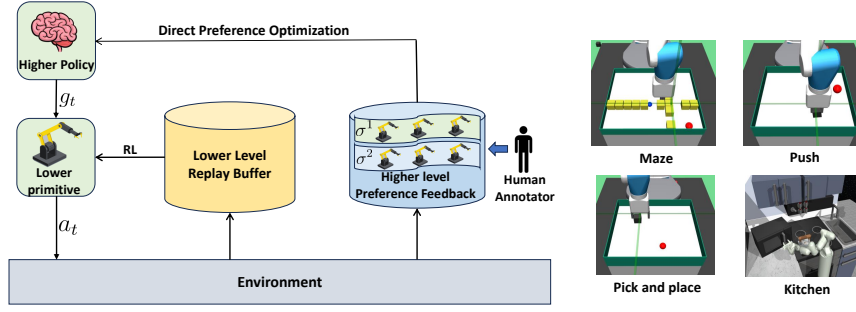


Figure 1: **DIPPER overview (left)**: The higher-level policy predicts subgoals g_t for the lower-level policy, which executes primitive actions a_t on the environment. The lower-level replay buffer is populated by environment interactions, and RL is subsequently used to optimize the lower-level policy. A human annotator is used to generate preference feedback data for the higher-level policy, and direct preference optimization is then used to learn the higher-level policy. **Training environments (right)**: (i) maze navigation, (ii) pick and place, (iii) push, and (iv) franka kitchen environment.

trained simultaneously. Concretely, due to continuously changing lower-level primitive behavior, the higher-level replay buffer experience is rendered obsolete. Some prior works deal with this issue by either simulating an optimal lower-level primitive [24], or relabeling replay buffer transitions using a maximum likelihood-based approach [26, 36]. In contrast, we deal with non-stationarity by using preference-based learning [6, 21]. Concretely, we first derive a primitive-regularized preference-based objective, and then directly optimize the higher-level policy by employing direct preference optimization [33]. Some other approaches use hand-designed action or behavior priors to boost downstream learning [29, 7]. While such approaches effectively simplify the learning process, performance in these approaches depends on the quality of the designed priors. If such priors are sub-optimal, the learning algorithm fails to show good performance. Another line of work uses the option learning framework [37, 18] to learn extended macro actions. However, such approaches may lead to degenerate solutions in the absence of suitable regularization. In contrast, our approach uses primitive-enabled regularization for conditioning the higher-level policy to produce feasible subgoals, thus avoiding such degenerate solutions.

Preference-based Learning. In this line of work, various approaches have been proposed that perform reinforcement learning (RL) on human preference data [19, 31, 40, 8]. Prior approaches first collect preference data from human annotators, then use this data for downstream learning. An important initial work in this area is [6], which first trains a reward model using the preference data, then uses RL to learn an optimal policy for the resulting reward model. Other recent work uses more sample-efficient off-policy policy gradient approaches [13] for learning the policy. Recently, direct preference optimization approach has been proposed [33, 32] that circumvents the reward model learning step, by directly optimizing the policy using a KL-regularized maximum likelihood objective. In this work, we propose a novel primitive-enabled reference policy, which directly optimizes the higher-level policy to generate feasible and achievable subgoals for the lower-level policy.

3 Problem Formulation

In this paper, we consider the Markov decision process (MDP) $(\mathcal{S}, \mathcal{A}, p, r, \gamma)$ framework, where \mathcal{S} is the state space, \mathcal{A} is the action space, $p : \mathcal{S} \times \mathcal{A} \rightarrow \Delta(\mathcal{S})$ is the transition probability function mapping state-action pairs to probability distributions over the state space, $r : \mathcal{S} \times \mathcal{A} \rightarrow \mathbb{R}$ is the reward function, and $\gamma \in (0, 1)$ is a discount factor. At timestep t , the agent is in state s_t , takes action $a_t \sim \pi(\cdot|s_t)$ according to some policy $\pi : \mathcal{S} \rightarrow \Delta(\mathcal{A})$ mapping states to probability distributions over the action space, receives reward $r_t = r(s_t, a_t)$, and the system transitions to a new state $s_{t+1} \sim p(\cdot|s_t, a_t)$. In the standard RL setting, the goal is to optimize the following objective:

$$\pi^* := \arg \max_{\pi} J(\pi) = \mathbb{E}_{\pi} \left[\sum_{t=0}^{\infty} \gamma^t r_t \right], \quad (1)$$

In what follows, we will consider the standard goal-conditioned setting [1], where the agent policy is jointly conditioned on the current state as well as a desired goal. Concretely, at timestep t , the policy π predicts actions $a_t \sim \pi(\cdot|s_t, g_t)$ conditioned on both state s_t and goal g_t . Finally, the value function for a policy π provides the expected cumulative reward when the start state is s_t and goal is g_t such that $V_\pi(s_t, g_t) = \mathbb{E}_\pi[\sum_{t=0}^T \gamma^t r_t | s_t, g_t]$.

3.1 Hierarchical Reinforcement Learning

In our goal-conditioned hierarchical setup, in order to achieve the end goal, the higher-level policy provides subgoals to the lower-level policy, while the lower-level policy takes primitive actions oriented towards achieving the specified subgoals. Concretely, the higher-level policy $\pi^H : \mathcal{S} \rightarrow \Delta(\mathcal{G})$ specifies a subgoal $g_t \in \mathcal{G}$, where $\mathcal{G} \subset \mathcal{S}$ is the set of possible goals. At each time step t , the higher-level policy predicts subgoal $g_t \sim \pi^H(\cdot|s_t)$ after every k timesteps and $g_t = g_{k \cdot \lceil t/k \rceil}$, otherwise. Thus, the higher-level policy issues new subgoals every k timesteps and keeps subgoals fixed in the interim.

Furthermore, at each t , the lower-level policy $\pi^L : \mathcal{S} \times \mathcal{G} \rightarrow \Delta(\mathcal{A})$ selects primitive actions $a_t \sim \pi^L(\cdot|s_t, g_t)$ according to the current state and subgoal specified by π^H , and the state transitions to $s_{t+1} \sim p(\cdot|s_t, a_t)$. Finally, the higher-level policy provides the lower level with reward $r_t^L = r^L(s_t, g_t, a_t) = -\mathbf{1}_{\{\|s_t - g_t\|_2 > \varepsilon\}}$, where $\mathbf{1}_B$ is the indicator function on a given set B . In the standard hierarchical RL setup, where both hierarchical levels are trained using RL, the higher level receives reward $r_t^H = r^H(s_t, g^*, g_t)$, where $g^* \in \mathcal{G}$ is the end goal and $r^H : \mathcal{S} \times \mathcal{G} \times \mathcal{G} \rightarrow \mathbb{R}$ is the higher-level reward function. The lower level populates its replay buffer with samples $(s_t, g_t, a_t, r_t^L, s_{t+1})$, while, at each t such that after every k timesteps, the higher level populates its buffer with samples of the form $(s_t, g^*, g_t, \sum_{i=t}^{t+k-1} r_i^H, s_{t+k})$. Next, we highlight key limitations of standard HRL methods.

3.1.1 Limitations of standard HRL approaches

Although HRL promises significant advantages over non-hierarchical RL, such as improvements in sample efficiency due to temporal abstraction and improved exploration [26, 27], it suffers from serious limitations. In this work, we focus on two outstanding issues:

L1: *training instability due to lower-level non-stationarity in off-policy HRL;*

L2: *performance degradation due to infeasible subgoal generation by higher-level policy.*

As discussed in [26] and [24], off-policy HRL suffers from non-stationarity due to non-stationary lower primitive behavior generated by the lower-level policy. Concretely, the higher-level replay transitions collected using previous lower-level policy become obsolete as the lower-level policy changes. Additionally, the higher level may predict infeasible subgoals to the lower-level policy [5], thus impeding learning and degrading overall performance. Hence, although standard HRL provides significant advantages, it often demonstrates poor performance in practice [26, 24, 5]. An important motivation of this work is to develop a novel preference-based learning approach that directly optimizes preference-based data to deal with the aforementioned limitations.

3.2 Classical RLHF Methods

In reinforcement learning from human feedback (RLHF) [39, 6, 21, 15], the agent first learns a reward model using human preference feedback, then learns a policy using RL that is optimal for the resulting reward model, typically via a policy gradient method such as PPO [35].

In this setting, the agent behavior over a k -length trajectory is represented as a sequence, τ , of state observations and actions: $\tau = ((s_t, a_t), (s_{t+1}, a_{t+1}) \dots (s_{t+k-1}, a_{t+k-1}))$. The reward model to be learned is represented as $\hat{r}_\phi : \mathcal{S} \times \mathcal{A} \rightarrow \mathbb{R}$, with parameters ϕ . Accordingly, the preferences between any two trajectories τ^1, τ^2 can be modeled using the Bradley-Terry model [3]:

$$P_\phi[\tau^1 \succ \tau^2] = \frac{\exp \sum_t \hat{r}_\phi(s_t^1, a_t^1)}{\sum_{i \in \{1, 2\}} \exp \sum_t \hat{r}_\phi(s_t^i, a_t^i)}, \quad (2)$$

where $\tau^1 \succ \tau^2$ implies that τ^1 is preferred over τ^2 . We consider the preference dataset \mathcal{D} with entries of the form (τ^1, τ^2, y) , where $y = (1, 0)$ when τ^1 is preferred over τ^2 , $y = (0, 1)$ when τ^2 is preferred over τ^1 , and $y = (0.5, 0.5)$ when there is no preference. The standard approach in the preference-based literature (see [6, 21]) is to learn the reward function \hat{r}_ϕ using the following

cross-entropy loss:

$$L(\phi) = - \sum_{\mathcal{D}} (y_1 \log P_{\phi} [\tau^1 \succ \tau^2] + y_2 \log P_{\phi} [\tau^2 \succ \tau^1]), \quad (3)$$

where $(\tau^1, \tau^2, y) \in \mathcal{D}$ and $y = [y_1, y_2]$.

3.3 Direct Preference Optimization

Unlike classical RLHF, direct preference optimization (DPO) circumvents the need for an RL algorithm by using a closed-form solution for the optimal policy of the KL-regularized RL problem [22, 41], which takes the form $\pi^*(a|s) = \frac{1}{Z(s)} \pi_{ref}(a|s) e^{r(s,a)}$, where π_{ref} is the reference policy, π^* is the optimal policy, and $Z(s)$ is a normalizing partition function ensuring that π^* provides a valid probability distribution over \mathcal{A} for each $s \in \mathcal{S}$. This formulation is rearranged to yield an alternative expression $r(s, a) = \alpha \log \pi^*(a|s) - \alpha \log \pi_{ref}(a|s) - Z(s)$ for the reward function. This equation is then substituted in the standard cross-entropy loss (3), which yields the following objective [33]:

$$\mathcal{L}_{DPO} = -\mathbb{E}_{(s, y_1, y_2) \sim \mathbb{D}} \left[\log \sigma \left(\alpha \log \frac{\pi_{\theta}(y_1|s)}{\pi_{ref}(y_1|s)} - \alpha \log \frac{\pi_{\theta}(y_2|s)}{\pi_{ref}(y_2|s)} \right) \right] \quad (4)$$

where θ are the policy parameters and $\sigma(x) = (1 + e^{-x})^{-1}$ denotes the sigmoid function.

4 Proposed Approach

In this section, we introduce DIPPER: **D**irect **P**reference Optimization to Accelerate **P**rimitive-**E**nabled Hierarchical **R**einforcement Learning. To address the problem of learning control problems for complex robotics tasks from human preference data, a natural approach is to apply a combination of RLHF and HRL: on the outer, highest tier a reward model is learned from the human preference data, on the middle tier RL is used to learn a corresponding higher-level policy for subgoal generation, and on the third, lowest tier RL is used to learn lower-level policies for achieving subgoals specified by the higher-level policy. Together, the lower and middle tiers in this approach naturally correspond to performing RLHF, while the middle and higher tiers correspond to performing HRL. Though intuitively reasonable, the need to carry out three distinct learning procedures simultaneously in this approach is computationally burdensome and a more efficient method is required.

Our key idea. The key idea underlying DIPPER is twofold: we introduce a DPO-based approach to directly learn higher-level policies from preference data, replacing the two-tier RLHF component in the scheme described above with a simpler, more efficient single-tier approach; we replace the reference policy inherent in DPO-based approaches, which is typically unavailable in complex robotics tasks, with a primitive-enabled reference policy derived from a novel bi-level optimization formulation of the HRL problem. The result is an efficient hierarchical approach that directly optimizes the higher-level policy using preference data while simultaneously mitigating the well-known non-stationarity and infeasible subgoal prediction problems of HRL (see Section 3.1.1) through primitive-enabled regularization.

The rest of this section proceeds as follows. We begin by providing the DPO-inspired objective from which our derivation of DIPPER originates. In order to address the reference policy issue mentioned above, we provide our novel bi-level optimization formulation of the HRL problem. Armed with this formulation, we introduce a corresponding reference policy and provide additional intuition underpinning it. We then proceed with our DPO-based derivation of the DIPPER objective. We end with some final remarks on practical implementation and provide an overview of the algorithm.

4.1 DIPPER

We now introduce our hierarchical approach DIPPER, which uses a primitive-enabled direct preference optimization formulation to optimize the higher-level policy and RL to optimize the lower-level policy. Recalling the HRL and RLHF settings of Sections 3.1 and 3.2, let $V_{\pi_L}(s_t, g_t)$ denote the lower-level value function and r_{ϕ} denote a parameterized reward model corresponding to the preference data. In addition, let $\alpha \geq 0$ be a scalar hyperparameter controlling the magnitude of the

KL-regularization term between higher level policy π_U and reference policy π_{ref} . For a trajectory τ of length T , we consider the following KL-regularized optimization problem:

$$\max_{\pi_U} \mathbb{E}_{\pi_U} \left[\sum_{t=0}^T (r_\phi(s_t, g_t) - \alpha \mathbb{D}_{\text{KL}}[\pi_U(\cdot|s_t) || \pi_{ref}(\cdot|s_t)]) \right] \quad (5)$$

In the standard DPO setting considered in [33, 32], the reference policy π_{ref} is assumed to be given. In challenging problems such as the robotics tasks motivating this work, however, such a reference policy is often unavailable. We must therefore seek an alternative reference policy corresponding to the HRL problem at hand. In order to achieve this, we next provide a novel bi-level formulation of the HRL problem that we will subsequently leverage to propose a suitable π_{ref} .

4.1.1 HRL: Bi-Level Optimization Formulation

We now present our bi-level optimization formulation of the HRL problem. For a given higher-level policy π_U , let π_L^* denote the corresponding optimal lower-level policy. Let $\tau = ((s_t, g_t), (s_{t+1}, g_{t+1}) \dots (s_{t+k-1}, g_{t+k-1}))$ represent the higher-level trajectories, where s_t is the State at time t , and $g_t \sim \pi_U(\cdot|s_t)$ is the subgoal predicted by the higher-level policy at time t . Notably, the higher-level policy π_U predicts the subgoal g_t for the lower-level policy, which is kept fixed for k timesteps while the lower level policy π_L^* executes. Hence, the next State s_{t+1} depends on the optimal lower-level policy π_L^* . We represent our hierarchical learning problem as the following bi-level optimization problem:

$$\max_{\pi_U} \mathcal{J}(\pi_U, \pi_L^*(\pi_U)) \quad \text{s.t.} \quad \pi_L^*(\pi_U) = \operatorname{argmax}_{\pi_L} V_{\pi_L}(\pi_U) \quad (6)$$

Note that, in the given constraint, the optimal lower-level policy π_L^* is defined as the policy which maximizes the lower-level value function V_{π_L} . We can solve this bi-level joint optimization for the higher-level policy. In order to optimize for both π_U and π_L , we reformulate (6) into the following value function formulation [25]:

$$\max_{\pi_U, \pi_L} \mathcal{J}(\pi_U, \pi_L) \quad \text{s.t.} \quad V_{\pi_L}(\pi_U) - V_{\pi_L}^*(\pi_U) \geq 0 \quad (7)$$

where, $V_{\pi_L}^*(\pi_U) = \max_{\pi_L} V_{\pi_L}(\pi_U)$. Notably, since the left-hand side of the inequality constraint is always non-positive due to the fact that $V_{\pi_L}(\pi_U) - V_{\pi_L}^*(\pi_U) \leq 0$, the constraint is satisfied only when $V_{\pi_L}(\pi_U) = V_{\pi_L}^*(\pi_U)$.

Finally, (7) can be formulated as the following Lagrangian objective:

$$\max_{\pi_U, \pi_L} \mathcal{J}(\pi_U, \pi_L) + \lambda (V_{\pi_L}(\pi_U) - V_{\pi_L}^*(\pi_U)) \quad (8)$$

We now use the bi-level formulation of HRL in equation (8) to propose a novel reference policy for our DPO-based objective. This yields an efficient HRL algorithm dealing with non-stationarity and infeasible subgoal generation that, as we will see in Section 5, is able to solve complex robotics tasks.

4.1.2 DIPPER Reference Policies

As discussed at the beginning of this section, a key component of the DPO-based approach is to provide a suitable reference policy, which may be difficult to obtain in the problems we consider. In light of the regularized objective (8) derived in Section 4.1.1, we propose the following formulation of the reference policy:

$$\pi_{ref}(g_t | s_t) = \frac{\exp(m(V_{\pi_L}(s_t, g_t) - V_{\pi_L}^*(s_t, g_t)))}{Z(s_t)} \quad (9)$$

where $Z(s_t) = \sum_{g_t} \exp(m(V_{\pi_L}(s_t, g_t) - V_{\pi_L}^*(s_t, g_t)))$, $V_{\pi_L}^*(s_t, g_t) = \max_{\pi_L} V_{\pi_L}(s_t, g_t)$, and $m = \frac{\lambda}{\alpha}$. Note that, since the term $V_{\pi_L}(s_t, g_t) - V_{\pi_L}^*(s_t, g_t)$ in the numerator is always non-positive, for a given g_t , the term is maximized when $V_{\pi_L}(s_t, g_t) = V_{\pi_L}^*(s_t, g_t)$. Equivalently, the term is maximized when, for a particular g_t , the lower-level value function is optimal. We show later on in Section 4.1.3 that, when this particular choice of reference policy is substituted in DPO objective, we get exactly the bi-level formulation in (8).

In addition to its connections to the bi-level optimization formulation, the specific form of the reference policy that we propose leads to significant advantages with respect to the hierarchical component of our approach. To see this, notice that the reference policy $\pi_{ref}(g_t | s_t)$ assigns high probability to the subgoal g_t , where the corresponding lower-level value function $V_{\pi_L}(s_t, g_t)$ is close to optimal, or alternatively, where the corresponding lower-level policy $\pi_L(s_t, g_t)$ is close to optimal. This formulation effectively handles the non-stationarity issue (**L1**) and infeasible subgoal generation issue (**L2**) in HRL as follows:

- **Dealing with L1:** For a particular subgoal g_t , if the lower-level policy is close to optimal, it predicts actions similar to the optimal lower-level policy. This reduces the non-stationary behavior of the lower-level policy, which ameliorates the non-stationarity issue in HRL.
- **Dealing with L2:** For a particular subgoal g_t , $V_{\pi_L}(s_t, g_t)$ provides an estimate of the achievability of subgoal g_t from current State s_t , since a high value of $V_{\pi_L}(s_t, g_t)$ implies that the lower level expects to achieve high reward for subgoal g_t . Since π_{ref} assigns high probability to subgoals with large $V_{\pi_L}(s_t, g_t)$, π_{ref} produces achievable subgoals, effectively dealing with infeasible subgoal generation issue in HRL.

4.1.3 DIPPER Objective

Here, we derive our DIPPER objective. We first substitute the proposed reference policy of (9) into the DPO objective (5) to get the following formulation:

$$\max_{\pi_U} \mathbb{E}_{\pi_U} \left[\sum_{t=0}^T (r_\phi(s_t, g_t) + \lambda(V_{\pi_L}(s_t, g_t) - V_{\pi_L}^*(s_t, g_t)) + \hat{m}(s_t)) \right], \quad (10)$$

where $\hat{m}(s_t) = (\alpha \mathcal{H}(s_t) - \alpha \log Z(s_t))$, and $\mathcal{H}(s_t) = -\log \pi_U(g_t | s_t)$ is the entropy term for higher-level policy. When optimizing for the higher-level policy, we can choose to ignore the term $\hat{m}(s_t)$, since it does not depend on the policy $\pi_U(g_t | s_t)$. Note that the formulation in (10) is exactly equal to the bi-level optimization formulation of (8). Hence, when we plug in the proposed form of primitive enabled reference policy (4.1.2) in KL-regularized DPO objective, this yields the bi-level optimization formulation in (8). Following prior work [22, 41] and substituting the reference policy in (5), we get the following optimal solution for the higher-level policy:

$$\pi_U(g_t | s_t) = \frac{1}{Z(s_t)} \exp\left(\frac{1}{\alpha} (r_\phi(s_t, g_t) + \lambda(V_{\pi_L}(s_t, g_t) - V_{\pi_L}^*(s_t, g_t)))\right), \quad (11)$$

where $Z(s_t) = \sum_{g_t} \exp(\frac{1}{\alpha} (r_\phi(s_t, g_t) + \lambda(V_{\pi_L}(s_t, g_t) - V_{\pi_L}^*(s_t, g_t))))$ is the partition function and λ is the primitive regularization weight hyper-parameter. Appendix A.1 contains a complete derivation. Taking logarithms on both sides of (11) and performing some elementary algebra yields

$$r_\phi(s_t, g_t) = \alpha \log Z(s_t) + \alpha \log \pi_U(g_t | s_t) - \lambda(V_{\pi_L}(s_t, g_t) - V_{\pi_L}^*(s_t, g_t)). \quad (12)$$

We can reformulate the Bradley-Terry preference model to derive the following objective:

$$\mathcal{L}^d = -\mathbb{E}_{(\tau_1, \tau_2) \sim \mathbb{D}} [\log \sigma(\sum_{t=0}^T r_\phi(s_t^1, g_t^1) - \sum_{t=0}^T r_\phi(s_t^2, g_t^2))] \quad (13)$$

We now substitute the preference reward formulation (12) into (13) to derive our final maximum likelihood objective:

$$\begin{aligned} \mathcal{L}^d = & -\mathbb{E}_{(\tau_1, \tau_2) \sim \mathbb{D}} [\log \sigma(\sum_{t=0}^T (\alpha \log \pi_U(g_t^1 | s_t^1) - \alpha \log \pi_U(g_t^2 | s_t^2)) - \\ & \lambda((V_{\pi_L}(s_t^1, g_t^1) - V_{\pi_L}^*(s_t^1, g_t^1)) - (V_{\pi_L}(s_t^2, g_t^2) - V_{\pi_L}^*(s_t^2, g_t^2)))] \end{aligned} \quad (14)$$

This objective provides the maximum likelihood DIPPER objective for optimizing the higher-level policy π_U while employing primitive-enabled regularization to predict feasible subgoals for the lower-level policy.

Analyzing DIPPER gradient: We further analyze the rationale behind the DIPPER objective by computing and interpreting the gradients of \mathcal{L}^d with respect to higher level policy π_U . The gradient

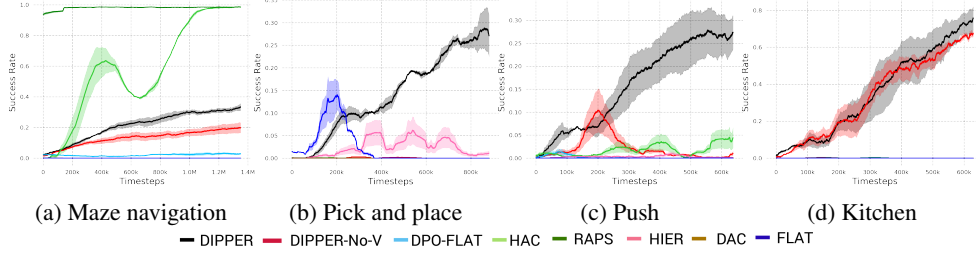


Figure 2: **Performance comparison** This figure compares the success rate performances on four sparse maze navigation and robotic manipulation tasks. The solid line and shaded regions represent the mean and standard deviation, across 5 seeds. We compare DIPPER against multiple baselines. As can be seen, although HAC and RAPS outperform DIPPER in maze task, DIPPER shows impressive performance and clearly outperforms the baselines in harder tasks.

can be written as:

$$\nabla \mathcal{L}^d = -\alpha \mathbb{E}_{(\tau_1, \tau_2) \sim \mathbb{D}} \left[\sum_{t=0}^T \underbrace{(\sigma(\hat{r}(s_t^2, g_t^2) - \hat{r}(s_t^1, g_t^1)))}_{\text{higher weight for wrong preference}} * \left[\underbrace{\nabla \log \pi_U(g_t^1 | s_t^1)}_{\text{increase likelihood of } \tau_1} - \underbrace{\nabla \log \pi_U(g_t^2 | s_t^2)}_{\text{decrease likelihood of } \tau_2} \right] \right] \quad (15)$$

where $\hat{r}(s_t, g_t) = \alpha \log \pi_U(g_t | s_t) - \lambda(V_{\pi_L}(s_t, g_t) - V_{\pi_L}^*(s_t, g_t))$ is the implicit reward defined by the higher-level policy and lower-level value function. Intuitively, the gradient term increases the likelihood of preferred trajectories and decreases the likelihood of trajectories that are not preferred. Notably, the examples are weighted by how incorrectly the implicit reward model $\hat{r}(s_t, g_t)$ orders the trajectories, according to the strength of the KL constraint.

4.1.4 DIPPER: A Practical algorithm

We now employ the derived DIPPER formulation to propose an efficient and practically applicable DPO-based algorithm. Notably, (14) requires calculation of optimal value function $V_{\pi_L}^*(s_t, g_t)$ for a subgoal g_t . Unfortunately, computing optimal value functions is computationally expensive and is typically not practically feasible. We accordingly consider an approximation $V_{\pi_L}^k(s_t, g_t)$ to replace $V_{\pi_L}^*(s_t, g_t)$, where k represents the number of training iterations for updating $V_L^k(s_t, g_t)$. We additionally make an approximation and ignore the term $V_{\pi_L}(s_t, g_t)$ in (14), yielding the following practically applicable maximum likelihood objective:

$$\mathcal{L}^d = -\mathbb{E}_{(\tau_1, \tau_2) \sim \mathbb{D}} \left[\log \sigma \left(\sum_{t=0}^T (\alpha \log \pi_U(g_t^1 | s_t^1) - \alpha \log \pi_U(g_t^2 | s_t^2)) + \lambda(V_L^k(s_t^1, g_t^1) - V_L^k(s_t^2, g_t^2)) \right) \right] \quad (16)$$

Despite these approximations, in our experiments we empirically find that DIPPER is able to efficiently mitigate the recurring issue of non-stationarity in HRL and generate feasible subgoals for the lower-level policy. We provide the DIPPER algorithm in Appendix A.3 Algorithm 1.

5 Experiments

In our empirical analysis, we ask the following questions: **(1)** Is DIPPER able to mitigate the recurring issue of non-stationarity in HRL? **(2)** Does DIPPER outperform flat direct preference optimization based approach? **(3)** Does DIPPER enhance sample efficiency and training stability in complex robotic manipulation and navigation tasks? **(4)** What is the contribution of each of our design choices?

5.1 Setup

We evaluate DIPPER on four robotic navigation and manipulation tasks: *(i)* maze navigation, *(ii)* pick and place [1], *(iii)* push, and *(iv)* franka kitchen [12]. These environments are sparse reward environments, where the lower primitive is sparsely rewarded when it comes within δ distance of the

subgoal. Unless explicitly stated, we keep these conditions consistent across all the baselines, to make sure the comparisons are fair. Notably, since the pick and place, push and kitchen task environments are complex sparse reward environments, we assume access to a single human demonstration, and use an additional imitation learning objective at the lower level. We do not assume access to any demonstration in the maze navigation task. This is done to speedup training, however, we keep this assumption consistent among all baselines to ascertain fair comparisons. We provide additional implementation details in Appendix A.5, and the implementation code in the supplementary.

5.2 Evaluation and Results

In our experimental analysis, we compare DIPPER against multiple hierarchical and non-hierarchical baselines: DIPPER-No-V (DIPPER without primitive-enabled regularization), DPO-FLAT (Single-level DPO implementation [33]), HIER (vanilla hierarchical SAC implementation), HAC (Hindsight Actor Critic [24]), DAC (Discriminator Actor Critic [20]), FLAT (Single-level SAC), and RAPS [7], in Figure 2. In order to illustrate the importance of primitive regularization employing lower primitive value function, we implement DIPPER-No-V baseline by removing primitive regularization from DIPPER. As seen from Figure 2, DIPPER performs slightly better than DIPPER-No-V in simpler maze navigation task and in kitchen task. However, DIPPER significantly outperforms DIPPER-No-V baseline in pick and place and push tasks. This clearly demonstrates the advantage of primitive regularization, which conditions the higher level policy to predict feasible subgoals. We also compare DIPPER against DPO-Flat, which is a single-level implementation of DPO [33]. We implemented this baseline to illustrate that our hierarchical DPO based approach (where the higher policy is trained using DPO based maximum likelihood objective, and the lower policy is trained using RL) outperforms single-level DPO based policy. Since DIPPER is hierarchical, it benefits from factors like temporal abstraction and improved exploration, which are missing from single-level DPO implementation. However, since we do not have access to a reference policy in robotics, we replace the reference policy with a uniform policy. Notably, this particular choice of reference policy effectively reformulates the KL-objective into an entropy maximization objective in DPO-Flat, which facilitates better exploration. DIPPER clearly outperforms this baseline in all the tasks, showing that our hierarchical structure is crucial for improved performance.

We also implemented Hierarchical Actor Critic [24], which deals with non-stationarity in HRL by simulating optimal lower primitive behavior. As seen in Figure 2, HAC is able to outperform DIPPER in simpler maze navigation task. However, in harder pick and place, push and kitchen tasks, DIPPER significantly outperforms this baseline, which shows that our DPO based hierarchical formulation better ameliorates non-stationarity in HRL. Further, we implemented HIER, which is vanilla HRL baseline implemented using SAC [13]. However, this baseline failed to perform well, especially in complex tasks. We also compared DIPPER with RAPS [7] baseline, to analyze how DIPPER performs against approaches that use behavior priors or action primitives. Notably, the performance of RAPS depends on the quality of such priors, and require considerable effort to hand-design, especially in hard environments like franka kitchen. We find that RAPS is able to significantly outperform DIPPER in maze task, which we believe is because the designed action primitive in maze task is near perfect. However, as the complexity of environments increase, RAPS is unable to show any progress. Finally, we implemented two single level baselines: Discriminator Actor Critic (DAC) [20] and FLAT baseline implemented using single level SAC. We provide one demonstration to DAC baseline in each environment. However, even with privileged information, DAC is unable to perform well. Similarly, FLAT baseline is unable to perform well, which shows that our hierarchical structure and primitive regularization are crucial for good performance in complex robotic tasks.

5.3 Ablation Analysis

Here, we perform the ablation analysis for selecting the hyper-parameters. The primitive regularization weight hyper-parameter λ directly controls the magnitude of primitive regularization. If λ is too small, we lose the advantages of primitive informed regularization. In contrast, if λ is too large, it may lead to degenerate solutions. We provide the ablation in Appendix A.4 Figure 3. Further, the hyper-parameter α controls the weight of KL constraint in higher level policy objective. If α is too large, the higher policy is very close to the reference policy, and if α is too small, the higher policy might stray too far from the reference policy, leading to poor performance in both scenarios. α thus controls the amount of KL regularization in the maximum likelihood DPO objective. We provide the ablation plots in Appendix A.4 Figure 4.

6 Conclusion

In this work, we propose DIPPER, a preference learning based HRL algorithm that employs direct policy optimization and primitive enabled regularization to mitigate the issues of non-stationarity and infeasible subgoal generation in HRL. We propose a bi-level optimization formulation for HRL and use it to propose a novel reference policy formulation which results in our primitive regularized maximum likelihood objective. We empirically show that DIPPER is able to demonstrate impressive performance on complex robotic control tasks, and is able to significantly outperform the baselines. Additionally, our hierarchical formulation is able to outperform single level DPO formulation. We provide the limitations and future work in Appendix A.6.

References

- [1] Marcin Andrychowicz, Filip Wolski, Alex Ray, Jonas Schneider, Rachel Fong, Peter Welinder, Bob McGrew, Josh Tobin, Pieter Abbeel, and Wojciech Zaremba. Hindsight experience replay. *CoRR*, abs/1707.01495, 2017. URL <http://arxiv.org/abs/1707.01495>.
- [2] Andrew G. Barto and Sridhar Mahadevan. Recent advances in hierarchical reinforcement learning. *Discrete Event Dynamic Systems*, 13:341–379, 2003.
- [3] Ralph Allan Bradley and Milton E. Terry. Rank analysis of incomplete block designs: I. the method of paired comparisons. *Biometrika*, 39:324, 1952. URL <https://api.semanticscholar.org/CorpusID:125209808>.
- [4] Zehong Cao, Kaichiu Wong, and Chin-Teng Lin. Human preference scaling with demonstrations for deep reinforcement learning. *arXiv preprint arXiv:2007.12904*, 2020.
- [5] Elliot Chane-Sane, Cordelia Schmid, and Ivan Laptev. Goal-conditioned reinforcement learning with imagined subgoals. In *International Conference on Machine Learning*, pages 1430–1440. PMLR, 2021.
- [6] Paul F Christiano, Jan Leike, Tom Brown, Miljan Martic, Shane Legg, and Dario Amodei. Deep reinforcement learning from human preferences. *Advances in neural information processing systems*, 30, 2017.
- [7] Murtaza Dalal, Deepak Pathak, and Russ R Salakhutdinov. Accelerating robotic reinforcement learning via parameterized action primitives. *Advances in Neural Information Processing Systems*, 34:21847–21859, 2021.
- [8] Christian Daniel, Oliver Kroemer, Malte Viering, Jan Metz, and Jan Peters. Active reward learning with a novel acquisition function. *Autonomous Robots*, 39:389–405, 2015.
- [9] Peter Dayan and Geoffrey E Hinton. Feudal reinforcement learning. *Advances in neural information processing systems*, 5, 1992.
- [10] Thomas G. Dietterich. Hierarchical reinforcement learning with the MAXQ value function decomposition. *CoRR*, cs.LG/9905014, 1999. URL <https://arxiv.org/abs/cs/9905014>.
- [11] Shixiang Gu, Ethan Holly, Timothy P. Lillicrap, and Sergey Levine. Deep reinforcement learning for robotic manipulation. *CoRR*, abs/1610.00633, 2016. URL <http://arxiv.org/abs/1610.00633>.
- [12] Abhishek Gupta, Vikash Kumar, Corey Lynch, Sergey Levine, and Karol Hausman. Relay policy learning: Solving long-horizon tasks via imitation and reinforcement learning. *arXiv preprint arXiv:1910.11956*, 2019.
- [13] Tuomas Haarnoja, Aurick Zhou, Pieter Abbeel, and Sergey Levine. Soft actor-critic: Off-policy maximum entropy deep reinforcement learning with a stochastic actor. *CoRR*, abs/1801.01290, 2018. URL <http://arxiv.org/abs/1801.01290>.
- [14] Jean Harb, Pierre-Luc Bacon, Martin Klissarov, and Doina Precup. When waiting is not an option: Learning options with a deliberation cost. In *Proceedings of the AAAI Conference on Artificial Intelligence*, volume 32, 2018.

- [15] Borja Ibarz, Jan Leike, Tobias Pohlen, Geoffrey Irving, Shane Legg, and Dario Amodei. Reward learning from human preferences and demonstrations in atari, 2018.
- [16] Dmitry Kalashnikov, Alex Irpan, Peter Pastor, Julian Ibarz, Alexander Herzog, Eric Jang, Deirdre Quillen, Ethan Holly, Mrinal Kalakrishnan, Vincent Vanhoucke, and Sergey Levine. Qt-opt: Scalable deep reinforcement learning for vision-based robotic manipulation. *CoRR*, abs/1806.10293, 2018. URL <http://arxiv.org/abs/1806.10293>.
- [17] Diederik P Kingma and Jimmy Ba. Adam: A method for stochastic optimization. *arXiv preprint arXiv:1412.6980*, 2014.
- [18] Martin Klissarov, Pierre-Luc Bacon, Jean Harb, and Doina Precup. Learnings options end-to-end for continuous action tasks. *arXiv preprint arXiv:1712.00004*, 2017.
- [19] W Bradley Knox and Peter Stone. Interactively shaping agents via human reinforcement: The tamer framework. In *Proceedings of the fifth international conference on Knowledge capture*, pages 9–16, 2009.
- [20] Ilya Kostrikov, Kumar Krishna Agrawal, Debidatta Dwibedi, Sergey Levine, and Jonathan Tompson. Discriminator-actor-critic: Addressing sample inefficiency and reward bias in adversarial imitation learning. *arXiv preprint arXiv:1809.02925*, 2018.
- [21] Kimin Lee, Laura Smith, and Pieter Abbeel. Pebble: Feedback-efficient interactive reinforcement learning via relabeling experience and unsupervised pre-training, 2021.
- [22] Sergey Levine. Reinforcement learning and control as probabilistic inference: Tutorial and review. *arXiv preprint arXiv:1805.00909*, 2018.
- [23] Sergey Levine, Chelsea Finn, Trevor Darrell, and Pieter Abbeel. End-to-end training of deep visuomotor policies. *CoRR*, abs/1504.00702, 2015. URL <http://arxiv.org/abs/1504.00702>.
- [24] Andrew Levy, George Konidaris, Robert Platt, and Kate Saenko. Learning multi-level hierarchies with hindsight. In *International Conference on Learning Representations*, 2018.
- [25] Bo Liu, Mao Ye, Stephen Wright, Peter Stone, and Qiang Liu. Bome! bilevel optimization made easy: A simple first-order approach. *Advances in neural information processing systems*, 35:17248–17262, 2022.
- [26] Ofir Nachum, Shixiang Shane Gu, Honglak Lee, and Sergey Levine. Data-efficient hierarchical reinforcement learning. *Advances in neural information processing systems*, 31, 2018.
- [27] Ofir Nachum, Haoran Tang, Xingyu Lu, Shixiang Gu, Honglak Lee, and Sergey Levine. Why does hierarchy (sometimes) work so well in reinforcement learning? *arXiv preprint arXiv:1909.10618*, 2019.
- [28] Ashvin Nair, Bob McGrew, Marcin Andrychowicz, Wojciech Zaremba, and Pieter Abbeel. Overcoming exploration in reinforcement learning with demonstrations. In *2018 IEEE international conference on robotics and automation (ICRA)*, pages 6292–6299. IEEE, 2018.
- [29] Soroush Nasiriany, Huihan Liu, and Yuke Zhu. Augmenting reinforcement learning with behavior primitives for diverse manipulation tasks. *CoRR*, abs/2110.03655, 2021. URL <https://arxiv.org/abs/2110.03655>.
- [30] Ronald Parr and Stuart Russell. Reinforcement learning with hierarchies of machines. In M. Jordan, M. Kearns, and S. Solla, editors, *Advances in Neural Information Processing Systems*, volume 10. MIT Press, 1998.
- [31] Patrick M Pilarski, Michael R Dawson, Thomas Degris, Farbod Fahimi, Jason P Carey, and Richard S Sutton. Online human training of a myoelectric prosthesis controller via actor-critic reinforcement learning. In *2011 IEEE international conference on rehabilitation robotics*, pages 1–7. IEEE, 2011.
- [32] Rafael Rafailov, Joey Hejna, Ryan Park, and Chelsea Finn. Your language model is secretly a q-function. *arXiv preprint arXiv:2404.12358*, 2024.

- [33] Rafael Rafailov, Archit Sharma, Eric Mitchell, Christopher D Manning, Stefano Ermon, and Chelsea Finn. Direct preference optimization: Your language model is secretly a reward model. *Advances in Neural Information Processing Systems*, 36, 2024.
- [34] Aravind Rajeswaran, Vikash Kumar, Abhishek Gupta, John Schulman, Emanuel Todorov, and Sergey Levine. Learning complex dexterous manipulation with deep reinforcement learning and demonstrations. *CoRR*, abs/1709.10087, 2017. URL <http://arxiv.org/abs/1709.10087>.
- [35] John Schulman, Filip Wolski, Prafulla Dhariwal, Alec Radford, and Oleg Klimov. Proximal policy optimization algorithms. *arXiv preprint arXiv:1707.06347*, 2017.
- [36] Utsav Singh, Wesley A Suttle, Brian M Sadler, Vinay P Namboodiri, and Amrit Singh Bedi. Piper: Primitive-informed preference-based hierarchical reinforcement learning via hindsight relabeling. *arXiv preprint arXiv:2404.13423*, 2024.
- [37] Richard S Sutton, Doina Precup, and Satinder Singh. Between mdps and semi-mdps: A framework for temporal abstraction in reinforcement learning. *Artificial intelligence*, 112(1-2): 181–211, 1999.
- [38] Alexander Sasha Vezhnevets, Simon Osindero, Tom Schaul, Nicolas Heess, Max Jaderberg, David Silver, and Koray Kavukcuoglu. Feudal networks for hierarchical reinforcement learning. In *International Conference on Machine Learning*, pages 3540–3549. PMLR, 2017.
- [39] Aaron Wilson, Alan Fern, and Prasad Tadepalli. A bayesian approach for policy learning from trajectory preference queries. In F. Pereira, C.J. Burges, L. Bottou, and K.Q. Weinberger, editors, *Advances in Neural Information Processing Systems*, volume 25. Curran Associates, Inc., 2012. URL https://proceedings.neurips.cc/paper_files/paper/2012/file/16c222aa19898e5058938167c8ab6c57-Paper.pdf.
- [40] Aaron Wilson, Alan Fern, and Prasad Tadepalli. A bayesian approach for policy learning from trajectory preference queries. *Advances in neural information processing systems*, 25, 2012.
- [41] Brian D Ziebart, Andrew L Maas, J Andrew Bagnell, Anind K Dey, et al. Maximum entropy inverse reinforcement learning. In *Aaai*, volume 8, pages 1433–1438. Chicago, IL, USA, 2008.

A Appendix

A.1 Deriving the final optimum of KL-Constrained Reward Maximization Objective

In this appendix, we will derive Eqn 11 from Eqn 5. Thus, we optimize the following objective:

$$\max_{\pi_U} \mathbb{E}_{\pi_U} \left[\sum_{t=0}^T (r_\phi(s_t, g_t) - \alpha \mathbb{D}_{\text{KL}}[\pi_U(g_t|s_t) \parallel \pi_{ref}(g_t|s_t)]) \right] \quad (17)$$

Re-writing the above equation after expanding KL divergence formula:

$$= \max_{\pi_U} \mathbb{E}_{\pi_U} \left[\sum_{t=0}^T (r_\phi(s_t, g_t) - \alpha \log \frac{\pi_U(g_t|s_t)}{\pi_{ref}(g_t|s_t)}) \right] \quad (18)$$

$$= \max_{\pi_U} \mathbb{E}_{\pi_U} \left[\sum_{t=0}^T (r_\phi(s_t, g_t) - \alpha \log \pi_U(g_t|s_t) + \alpha \log \pi_{ref}(g_t|s_t)) \right] \quad (19)$$

Substituting π_{ref} from Eqn 9, and $m = \frac{\lambda}{\alpha}$ in Equation 19,

$$\begin{aligned} &= \max_{\pi_U} \mathbb{E}_{\pi_U} \left[\sum_{t=0}^T (r_\phi(s_t, g_t) - \alpha \log \pi_U(g_t|s_t) + \alpha \log \exp(k(V_L(s_t, g_t) - V_L^*(s_t, g_t))) \right. \\ &\quad \left. - \alpha \log \sum_{g_t} \exp(k(V_L(s_t, g_t) - V_L^*(s_t, g_t))) \right] \end{aligned} \quad (20)$$

$$\begin{aligned} &= \max_{\pi_U} \mathbb{E}_{\pi_U} \left[\sum_{t=0}^T (r_\phi(s_t, g_t) - \alpha \log \pi_U(g_t|s_t) + \lambda(V_L(s_t, g_t) - V_L^*(s_t, g_t))) \right. \\ &\quad \left. - \alpha \log \sum_{g_t} \exp(k(V_L(s_t, g_t) - V_L^*(s_t, g_t))) \right] \end{aligned} \quad (21)$$

$$\begin{aligned} &= \min_{\pi_U} \mathbb{E}_{\pi_U} \left[\sum_{t=0}^T (\log \pi_U(g_t|s_t) - \frac{1}{\alpha} (r_\phi(s_t, g_t) + \lambda(V_L(s_t, g_t) - V_L^*(s_t, g_t))) \right. \\ &\quad \left. + \log \sum_{g_t} \exp(k(V_L(s_t, g_t) - V_L^*(s_t, g_t))) \right] \end{aligned} \quad (22)$$

$$\begin{aligned} &= \min_{\pi_U} \mathbb{E}_{\pi_U} \left[\sum_{t=0}^T (\log \left(\frac{\pi_U(g_t|s_t)}{\exp(\frac{1}{\alpha} (r_\phi(s_t, g_t) + \lambda(V_L(s_t, g_t) - V_L^*(s_t, g_t)))} \right) \right. \\ &\quad \left. + \log \sum_{g_t} \exp(k(V_L(s_t, g_t) - V_L^*(s_t, g_t))) \right] \end{aligned} \quad (23)$$

$$\begin{aligned} &= \min_{\pi_U} \mathbb{E}_{\pi_U} \left[\sum_{t=0}^T (\log \left(\frac{\pi_U(g_t|s_t)}{\frac{1}{Z(s)} \exp(\frac{1}{\alpha} (r_\phi(s_t, g_t) + \lambda(V_L(s_t, g_t) - V_L^*(s_t, g_t)))} \right) \right. \\ &\quad \left. + \log \sum_{g_t} \exp(k(V_L(s_t, g_t) - V_L^*(s_t, g_t))) - \log Z(s) \right] \end{aligned} \quad (24)$$

where, $Z(s) = \sum_{g_t} \exp(\frac{1}{\alpha}(r_\phi(s_t, g_t) + \lambda(V_L(s_t, g_t) - V_L^*(s_t, g_t))))$

Note that the partition function $Z(s)$ and the term $\log \sum_{g_t} \exp(k(V_L(s_t, g_t) - V_L^*(s_t, g_t)))$, do not depend on the policy π_U

$$= \min_{\pi_U} \mathbb{E}_{\pi_U} [\sum_{t=0}^T (\mathbb{D}_{\text{KL}}[\pi_U(g_t|s_t) \parallel \pi_U^*(g_t|s_t)] - \log \sum_{g_t} \exp(k(V_L(s_t, g_t) - V_L^*(s_t, g_t))) - \log Z(s))] \quad (25)$$

where, $\pi_U^*(g_t|s_t) = \frac{1}{Z(s)} \exp(\frac{1}{\alpha}(r_\phi(s_t, g_t) + \lambda(V_L(s_t, g_t) - V_L^*(s_t, g_t))))$ which is a valid probability distribution. $\pi_U^*(g_t|s_t)$ is minimized when, $D_{\text{KL}} = 0$. Hence,

$$\pi_U(g_t|s_t) = \pi_U^*(g_t|s_t) = \frac{1}{Z(s)} \exp(\frac{1}{\alpha}(r_\phi(s_t, g_t) + \lambda(V_L(s_t, g_t) - V_L^*(s_t, g_t)))) \quad (26)$$

A.2 Implementation details

We perform the experiments on two system each with Intel Core i7 processors, equipped with 48GB RAM and Nvidia GeForce GTX 1080 GPUs. We also provide the timesteps taken for running the experiments. For environments (i) – (iv), the maximum task horizon \mathcal{T} is set to 225, 50, 50, 225 timesteps, respectively, and the lower primitive is allowed to execute for 15, 7, 7 and 15 timesteps, respectively. In our experiments, we use off-policy Soft Actor Critic (SAC) [13] for optimizing RL objective, using the Adam [17] optimizer. The actor and critic networks are formulated as three-layer, fully connected neural networks with 512 neurons in each layer. The experiments are run for 1.35e6, 9e5, 1.3E6, and 6.3e5 timesteps in environments (i) – (iv), respectively. In the maze navigation task, a 7-degree-of-freedom (7-DoF) robotic arm traverses a four-room maze, with its closed gripper (fixed at table height) maneuvering through the maze to reach the goal position. For the pick and place task, the 7-DoF robotic arm gripper must locate a square block, pick it up, and deliver it to the goal position. In the push task, the 7-DoF robotic arm gripper is required to push the square block toward the goal position. In the kitchen task, a 9-DoF Franka robot must execute a pre-defined complex task to achieve the final goal, specifically, opening the microwave door. We compare our approach to the Discriminator Actor-Critic [20], which is provided with a single expert demonstration. Although not explored here, combining preference-based learning and learning from demonstrations presents an intriguing research direction [4].

To ensure fair comparisons, we maintain consistency across all baselines by keeping parameters such as neural network layer width, number of layers, choice of optimizer, SAC implementation parameters, etc., the same wherever possible. In RAPS, the lower-level behaviors are as follows: for maze navigation, we design a single primitive, *reach*, where the lower-level primitive moves in a straight line towards the subgoal predicted by the higher level. For the pick and place and push tasks, we design three primitives: *gripper-reach*, where the gripper moves to a specified position (x_i, y_i, z_i) ; *gripper-open*, which opens the gripper; and *gripper-close*, which closes the gripper. In the kitchen task, we use the action primitives implemented in RAPS [7].

A.2.1 Additional hyper-parameters

Here, we enlist the additional hyper-parameters used in DIPPER:

```
activation: tanh [activation for reward model]
layers: 3 [number of layers in the critic/actor networks]
hidden: 512 [number of neurons in each hidden layers]
Q_lr: 0.001 [critic learning rate]
pi_lr: 0.001 [actor learning rate]
buffer_size: int(1E7) [for experience replay]
clip_obs: 200 [clip observation]
n_cycles: 1 [per epoch]
n_batches: 10 [training batches per cycle]
batch_size: 1024 [batch size hyper-parameter]
```


reward_batch_size: 50 [reward batch size for DPO-FLAT]
 random_eps: 0.2 [percentage of time a random action is taken]
 alpha: 0.05 [weightage parameter for SAC]
 noise_eps: 0.05 [std of gaussian noise added to not-completely-random actions]
 norm_eps: 0.01 [epsilon used for observation normalization]
 norm_clip: 5 [normalized observations are cropped to this values]
 adam_beta1: 0.9 [beta 1 for Adam optimizer]
 adam_beta2: 0.999 [beta 2 for Adam optimizer]

A.3 DIPPER Algorithm

Here, we provide the psuedo-code for DIPPER algorithm

Algorithm 1 DIPPER

```

1: Initialize preference dataset  $\mathcal{D} = \{\}$ 
2: Initialize lower level replay buffer  $\mathcal{R}^L = \{\}$ 
3: for  $i = 1 \dots N$  do
4:   // Collect higher level trajectories  $\tau$  using  $\pi^H$  and lower level trajectories  $\rho$  using  $\pi^L$ ,
5:   // and store the trajectories in  $\mathcal{D}$  and  $\mathcal{R}^L$  respectively
6:   // After every g timesteps, relabel  $\mathcal{D}$  using human preference feedback  $y$ 
7:   // Lower level value function update
8:   for each gradient step in  $t=0$  to  $k$  do
9:     Optimize lower level value function  $V_{\pi^L}$  to get  $V_{\pi^L}^k$ 
10:  // Higher level policy update using DIPPER
11:  for each gradient step do
12:    // Sample higher level behavior trajectories
13:     $(\tau^1, \tau^2, y) \sim \mathcal{D}$ 
14:    Optimize higher level policy  $\pi^U$  using (16)
15:  // Lower primitive policy update using RL
16:  for each gradient step do
17:    Sample  $\rho$  from  $\mathcal{R}^L$ 
18:    Optimize lower policy  $\pi^L$  using SAC
  
```

A.4 Ablation Experiments

Here, we provide the plots for the ablation experiments.

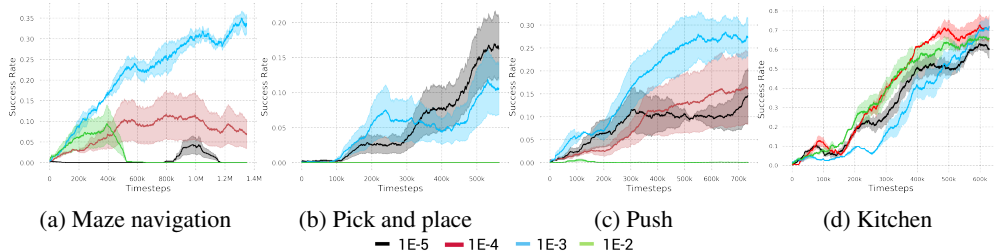


Figure 3: Regularization hyper-parameter ablation This figure compares the success rate performances for various values of primitive regularization weight λ hyper-parameter. If α is too small, we lose the advantages of primitive informed regularization, leading to poor performance. In contrast, if α is too large, it may lead to degenerate solutions. Thus, picking proper λ value is crucial for appropriate subgoal prediction, and improving overall performance.

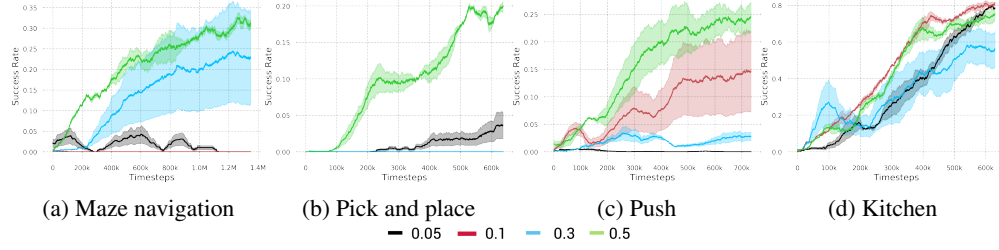


Figure 4: **KL weight hyper-parameter ablation** This figure compares the success rate performances for various values of KL weight α hyper-parameter. This hyper-parameter value controls the weight of KL constraint in higher-level policy objectives. If α is too large, the higher policy is very close to the reference policy, and if α is too small, the higher policy is far from the reference policy. We pick the hyper-parameter values after extensive ablation experiments.

A.5 Environment details

A.5.1 Maze navigation task

In this environment, a 7-DOF robotic arm gripper navigates through randomly generated four-room mazes. The gripper remains closed, and the positions of walls and gates are generated randomly. The table is discretized into a rectangular $W \times H$ grid, with vertical and horizontal wall positions W_P and H_P randomly selected from $(1, W - 2)$ and $(1, H - 2)$, respectively. In the constructed four-room environment, the four gate positions are randomly chosen from $(1, W_P - 1)$, $(W_P + 1, W - 2)$, $(1, H_P - 1)$, and $(H_P + 1, H - 2)$. The height of the gripper is fixed at table height, and it must navigate through the maze to reach the goal position, indicated by a red sphere.

The following implementation details apply to both the higher and lower-level policies unless explicitly stated otherwise. The environment features continuous state and action spaces. The state is represented as the vector $[p, \mathcal{M}]$, where p is the current gripper position, and \mathcal{M} is the sparse maze array. The higher-level policy input is a concatenated vector $[p, \mathcal{M}, g]$, where g is the target goal position. In contrast, the lower-level policy input is a concatenated vector $[p, \mathcal{M}, s_g]$, where s_g is the sub-goal provided by the higher-level policy. The current position of the gripper is considered the current achieved goal. The sparse maze array \mathcal{M} is a discrete 2D one-hot vector array, where a value of 1 indicates the presence of a wall block, and 0 indicates its absence. In our experiments, the sizes of p and \mathcal{M} are set to 3 and 110, respectively. The higher-level policy predicts sub-goal s_g , so its action space dimension matches the goal space dimension of the lower primitive. The lower primitive action a , directly executed in the environment, is a 4-dimensional vector with each dimension $a_i \in [0, 1]$. The first three dimensions provide offsets to be scaled and added to the gripper position for movement. The last dimension controls the gripper: 0 implies fully closed, 0.5 implies half-closed, and 1 implies fully open.

A.5.2 Pick and place and Push Environments

In the pick and place environment, a 7-DOF robotic arm gripper must pick up a square block and place it at a goal position set slightly above table height. This complex task requires the gripper to navigate to the block, close the gripper to grasp the block, and then move the block to the desired goal position. In the push environment, the 7-DOF robotic arm gripper needs to push a square block towards the goal position. The state is represented as the vector $[p, o, q, e]$, where p is the current gripper position, o is the position of the block on the table, q is the relative position of the block to the gripper, and e consists of the linear and angular velocities of both the gripper and the block. The higher-level policy input is thus a concatenated vector $[p, o, q, e, g]$, where g is the target goal position. The lower-level policy input is a concatenated vector $[p, o, q, e, s_g]$, where s_g is the sub-goal provided by the higher-level policy. The current position of the block is considered the current achieved goal. In our experiments, the sizes of p , o , q , and e are set to 3, 3, 3, and 11, respectively. The higher-level policy predicts sub-goal s_g , so the action space and goal space dimensions are the same. The lower primitive action a is a 4-dimensional vector with each dimension $a_i \in [0, 1]$. The first three dimensions provide offsets for the gripper position, and the last dimension controls the gripper (0 for closed and 1 for open). During training, the positions of the block and goal are randomly generated, with the block always starting on the table and the goal always above the table at a fixed height.

A.6 Limitations and future work

Our DPO based hierarchical formulation raises an important question. Since DIPPER employs DPO for training the higher level policy, does it generalize on out of distribution states and actions, as compared with learning from reward model based RL formulation. A direct comparison with hierarchical RLHF based formulation might provide interesting insights. Additionally, it will be challenging to apply DIPPER in scenarios where the subgoal space is high dimensional. These are interesting research avenues, and we leave further analysis for future work.

A.7 Impact Statement

Our proposed approach and algorithm are not expected to lead to immediate technological advancements. Instead, our primary contributions are conceptual, focusing on fundamental aspects of Hierarchical Reinforcement Learning (HRL). By introducing a preference-based methodology, we offer a novel framework that we believe has significant potential to enhance HRL research and its related fields. This conceptual foundation paves the way for future investigations and could stimulate advancements in HRL and associated areas.

A.8 Environment visualizations

Here, we provide some visualizations of the agent successfully performing the task.

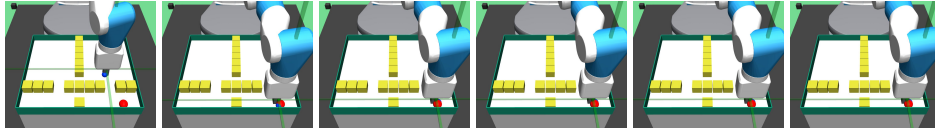


Figure 5: **Maze navigation task visualization:** The visualization is a successful attempt at performing maze navigation task

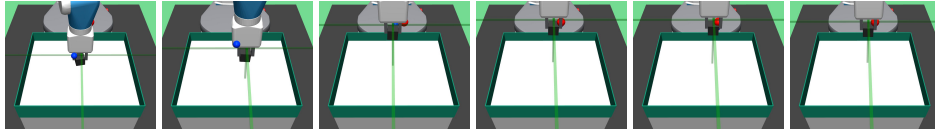


Figure 6: **Pick and place task visualization:** This figure provides visualization of a successful attempt at performing pick and place task

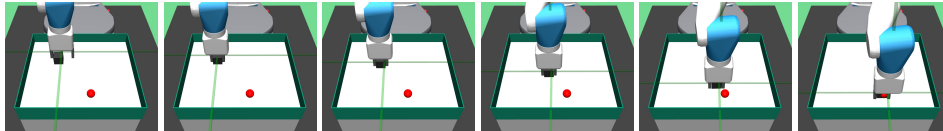


Figure 7: **Push task visualization:** The visualization is a successful attempt at performing push task



Figure 8: **Kitchen task visualization:** The visualization is a successful attempt at performing kitchen task